Journal of Alloys and Compounds 505 (2010) 343–347

Contents lists available at ScienceDirect

Journal of Alloys and Compounds

journal homepage: www.elsevier.com/locate/jallcom

Thermodynamic destabilization of Li–N–H system by Si addition

P. Palade*, G.A. Lungu, A.M. Husanu

National Institute of Materials Physics, Atomistilor Str. 105 bis, 077125 Magurele, Romania

ARTICLE INFO

Article history:
Received 16 November 2009
Received in revised form 26 March 2010
Accepted 31 March 2010
Available online 18 June 2010

Keywords:
Hydrogen absorbing materials
Mechanical alloying
Thermochemistry
X-ray diffraction

ABSTRACT

Li–N–H and Li–Si–N–H composites have been synthesized by ball milling starting from lithium amide, lithium hydride and silicon powders. Hydrogen sorption behaviour was investigated for the Si-containing composites and a Li–N–H reference sample. The as-milled Si-containing sample showed the presence of the constituent powders but after few absorption–desorption cycles an important amount of Li_2SiN_2 appeared in both de-hydrogenated and re-hydrogenated composites. This phase was present in higher amount in the de-hydrogenated sample than in the re-hydrogenated one. The presence of this phase was also confirmed by XPS measurements. Li–N–H and Li–Si–N–H composites in de-hydrogenated state also contained lithium imide. X-ray diffraction data indicated a reversible hydrogen generating reaction between lithium amide, lithium hydride and silicon to produce Li_2SiN_2, lithium imide and hydrogen. The plateau pressure of Li–N–Si–H system is twice the one for Li–N–H at the same temperature (about 265 °C), as shown by pressure–composition isotherms in desorption mode. For the first time it has been observed a thermodynamic destabilization of Li–N–H by mixing it with Si.

1. Introduction

Lithium-based materials are very promising for hydrogen storage purpose due to the very high content of hydrogen by weight (wt% H_2). Lithium alanates [1], borohydrides [2] and amides [3] have been studied extensively. The amides have been proposed as hydrogen storage materials since 2003 [4]. Their main problem was the progressive loss of hydrogen storage capacity due to ammonia (NH_3) release, but it has been found that by mixing lithium amide ($LiNH_2$) and lithium hydride (LiH) the loss of storage capacity can be substantially reduced below 350 °C [5]. The mechanism of suppression of NH_3 release has been intensively studied and it seems that the explanation is an ultra-fast reaction between LiH and NH_3 to produce H_2 and lithium imide (Li_2NH) [6].

By the reaction

$$LiNH_2 + LiH \leftrightarrow Li_2NH + H_2 \quad (1)$$

an amount of theoretically 6.5 wt% H_2 can be reversibly stored. Even if the desorbed hydrogen amount is relatively high, the plateau pressure of the pressure–composition isotherm (PCI) in desorption mode is small at temperatures of interest. Thermodynamic destabilization of LiH (increase of plateau pressure compared to LiH reference system) has been observed for the LiH + Si mixture for the first time by Vajo and Olson [7]. Another important result has been the destabilization of $LiNH_2$ by magnesium hydride (MgH_2) addition [8]. Mixture of amides and hydrides [9,10], amides and borohydrides [11], amides and alanates [12] have been prepared and investigated during the last few years and in some cases destabilization effects were also observed. According to our knowledge, no thermodynamic destabilization has been reported by mixing $LiNH_2$ with transition metals, C or Si. In the present work we have prepared Li–N–H–Si composites to study the possibility of destabilization effect of Si on the Li–N–H system. The stoichiometry of the prepared composites envisaged the reaction:

$$3LiNH_2 + 2LiH + Si \leftrightarrow Li_5SiN_3 + 4H_2 \quad (2)$$

with a theoretically amount of 7.14 wt% of released H_2.

2. Experimental

The starting materials, $LiNH_2$ (Alfa Aesar, 95%), LiH (Alfa Aesar, 99.4%), Si (Alfa Aesar, 99.9%), were milled together in RETSCH-400 PM planetary mill with vial and spheres made by tempered chromium steel. The proportion between the starting powders was $3LiNH_2$:2LiH:Si and the ball to powder ratio was 20:1. A reference sample (R-sample) was obtained by milling $LiNH_2$:LiH. Short times (5 min) of pause were intercalated between each 15 min milling reprises resulting in a total effective milling time of 72 h. The sample manipulation was done into a MBraun glove box under purified Argon (<1 ppm O_2, <1 ppm H_2O) in all the stages of the work. The milling atmosphere was the purified Ar at the small overpressure of the glove box (1.014 bar).

X-ray diffraction measurements were performed for the as-milled, de-hydrogenated and re-hydrogenated samples using a D-8 Advance Bruker diffractometer with Cu-Kα radiation. The samples were covered with a thin polymeric layer in order to avoid oxidation during XRD measurements.

X-ray photoelectron spectroscopy (XPS) measurements were performed in a dedicated photoemission chamber (Specs, Germany). An Al Kα monochromatized X-ray source (1486.74 eV) was used. Prior to XPS analysis, surface contamination was removed by 10 μA/cm² 4 keV Ar^+ sputtering for 30 min.

* Corresponding author. Tel.: +40 21 3690185; fax: +40 21 3690177.
E-mail address: palade@infim.ro (P. Palade).

0925-8388/$ – see front matter © 2010 Elsevier B.V. All rights reserved.
doi:10.1016/j.jallcom.2010.03.249

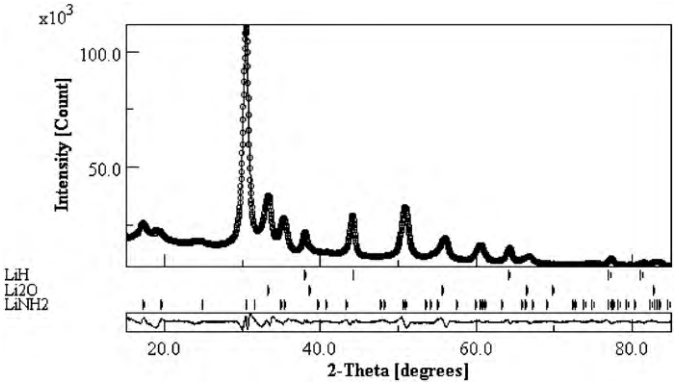

Fig. 1. Rietveld refinements for $LiNH_2$ + LiH as-milled sample.

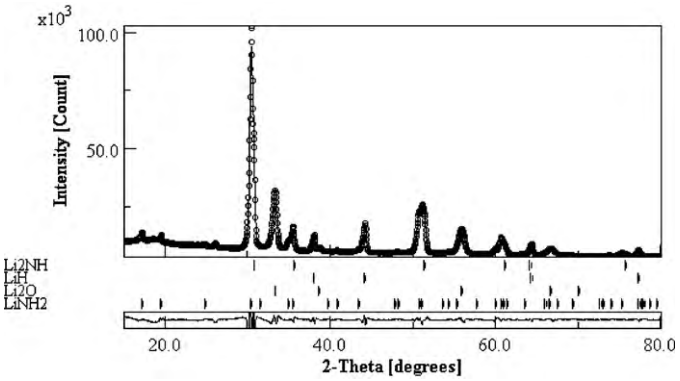

Fig. 2. Rietveld refinements for $LiNH_2$ + LiH re-hydrogenated sample.

In order to compensate from the sample surface charging, an electron flood gun operating at 1 eV acceleration energy and 0.1 mA electron current was used.

Thermal programmed desorption measurements (TPD) and pressure–composition isotherms in desorption mode (PCI des) were obtained using a commercially available volumetric Sievert apparatus provided by Advanced Material Corporation, Pittsburgh, USA. Hydrogen evacuation from samples was done using a dual stage rotary pump (ultimate pressure 10^{-3} Torr). The pressure sensors had a resolution of 0.2 bar. Due to the instrument limitations, the PCI des measurements were performed down to only 0.1 bar. This is not real impediment because the fuel cells require hydrogen pressures of at least 1 bar.

3. Results and discussion

As shown by X-ray diffraction profile of Fig. 1 the as-milled R-sample contains only $LiNH_2$, LiH and Li_2O. The peaks are broad, indicating small crystallites. The Rietveld refinement (also presented in Fig. 1), obtained with the MAUD software [13] indicates some misfit at about $2\theta = 19^\circ$ due to amorphous contribution of the polymer film covering the sample holder. The estimated crystal sizes are 16(2) nm for $LiNH_2$, 12(2) nm for Li_2O and 29(2) nm for LiH. For the most evident phase ($LiNH_2$), the crystallite size obtained using the MAUD software was checked against the Williamson–Hall plot and the results are in very good agreement. After five hydrogen absorption–desorption cycles, the XRD pattern of the re-hydrogenated R-sample (Fig. 2) exhibits the same phases ($LiNH_2$, LiH and Li_2O) but the peaks are sharper, clearly indicating crystallites increase. Also a very small amount of lithium imide (Li_2NH) was detected. The Rietveld refinement (Fig. 2) for the re-hydrogenated R-sample gives crystal sizes 2–3 times larger than for the as-ball milled R-sample: 47(3) nm for $LiNH_2$, 38(3) nm for Li_2O and 50(4) nm for LiH. This crystallite size increase is also supported by scanning electron microscopy (SEM). However, the accuracy of SEM measurements (not reported) is influenced by oxidation during sample manipulation in air. The XRD pattern of the de-hydrogenated R-sample (Fig. 3) shows the presence of Li_2NH and Li_2O. The Rietveld refinement for this sample gives a very large crystal size of 67(4) nm for Li_2NH as shown in the same figure.

In Table 1 is given a comparison between the lattice parameters of the crystalline phases for as-ball milled, re-hydrogenated and de-hydrogenated R-samples, as derived with the MAUD software and the same parameters from literature (ICDD database). In the same table there are presented also the reliability refinement parameters: GOF (goodness of fit), R_p, R_{wp}. The GOF values vary in the range 2.35–3.05 while R_{wp} does not exceed 6%.

Interestingly, excepting $LiNH_2$ which is tetragonal, all the other phases are face centered cubic. LiH has the same lattice parameter for both ball milled and re-hydrogenated samples within the error bar. $LiNH_2$ phase in ball milled R-sample has a larger lattice parameter than in re-hydrogenated sample. The refined lattice parameter of Li_2O from the de-hydrogenated R-sample is the same as for re-hydrogenated R-sample. The refined lattice parameters of $LiNH_2$ and Li_2O from as-ball milled and re-hydrogenated R-sample are larger than those given in literature (belonging to the same phases but in bulk form). It seems that ball milling causes this enhancement, as expectedly for very small crystallites. The lattice parameters of LiH phase in the re-hydrogenated R-sample and of Li_2NH in the de-hydrogenated R-sample fit well the

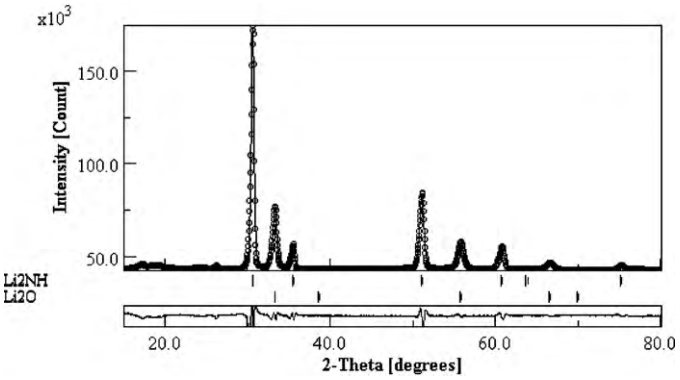

Fig. 3. Rietveld refinements for $LiNH_2$ + LiH de-hydrogenated sample.

Table 1
Lattice parameters and the reliability parameters of the fit (GOF, R_p, R_{wp}) obtained from Rietveld refinements for as-ball milled, re-hydrogenated and de-hydrogenated $LiNH_2$ + LiH R-samples.

Crystalline phase	Space group	As-ball milled sample (GOF = 2.87, R_p = 2.98%, R_{wp} = 3.88%)	Re-hydrogenated sample (GOF = 3.05, R_p = 4.38%, R_{wp} = 5.77%)	De-hydrogenated sample (GOF = 2.34, R_p = 1.18% R_{wp} = 2.44%)	Literature data
$LiNH_2$	*I*-4	a = 0.5071(3) nm c = 1.0258(5) nm	a = 0.5060(3) nm c = 1.0262(5) nm	Not present	a = 0.5016 nm c = 1.0220 nm
Li_2O	*Fm*-3*m*	a = 0.4662(3) nm	a = 0.4655(3) nm	a = 0.4657(3) nm	a = 0.4619 nm
LiH	*Fm*-3*m*	a = 0.4103(3) nm	a = 0.4097(3) nm	Not present	a = 0.4096 nm
Li_2NH	*Fm*-3*m*	Not present	a = 0.5040(3) nm	a = 0.5051(3) nm	a = 0.5047 nm

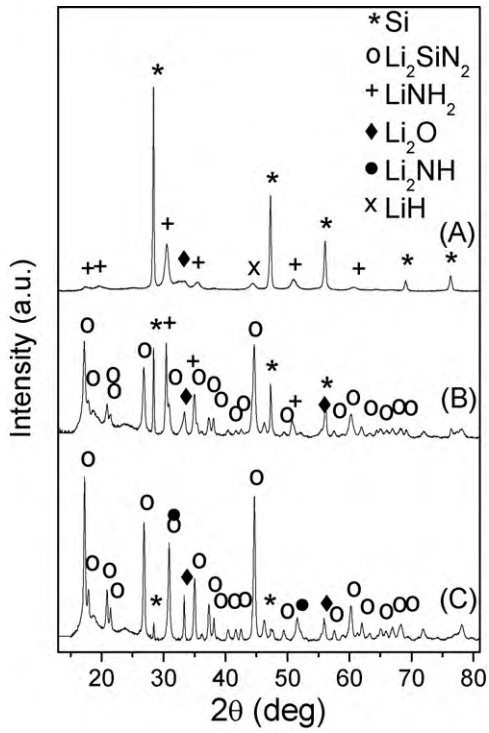

Fig. 4. X-ray diffraction data of 3LiNH:2LiH:Si samples (A – as-milled, B – re-hydrogenated, C – de-hydrogenated).

literature data and these phases are the closest to the corresponding bulk phase, in agreement with the observed large crystallite size.

The quantitative analysis for as-ball milled and re-hydrogenated R-samples gives good results for the 1:1 ratio between $LiNH_2$ and LiH. Additionally, about 14 wt% of Li_2O appears in all three samples and in the re-hydrogenated R-sample 10 wt% Li_2NH is also present. Most probably Li_2O is formed during the XRD measurements.

The XRD pattern of the as-milled Si-sample (with $3LiNH_2$:2LiH:Si proportion) shows broad peaks of $LiNH_2$, LiH, Li_2O, and peaks of Si which dominate the diagram (Fig. 4A). This is not only due to the higher X-ray scattering factor but also to the large crystal size of Si which gives narrow peaks. The XRD pattern of the re-hydrogenated Si-sample (Fig. 4B) shows the presence of Li_2SiN_2, $LiNH_2$, Li_2O and Si phases. The peaks belonging to Li_2SiN_2 are the most evident. Fig. 4C is the XRD pattern of the de-hydrogenated Si-sample, which displays the presence of Li_2NH in place of $LiNH_2$. Both de-hydrogenated and re-hydrogenated Si-samples contain some amorphous phase at 2θ of about 18° and 24°. This contribution is relatively important and cannot be originated by the thin polymer film covering the sample holder. The amount of Si present in the de-hydrogenated Si-sample is much lower than in the re-hydrogenated sample and the Li_2SiN_2 contribution is higher in de-hydrogenated Si-sample than in the same sample in re-hydrogenated state. Taking into account the modifications of the amount of crystalline phases discussed above, the XRD data for the re-hydrogenated and de-hydrogenated Si-samples suggest the following hydrogen generating reaction:

$$(u+1)LiNH_2 + uLiH + (1/2)Si \leftrightarrow uLi_2NH + (1/2)Li_2SiN_2 + (u+1)H_2. \quad (3)$$

LiH cannot be clearly distinguished in the XRD pattern of the re-hydrogenated Si-sample due to overlapping with the Li_2SiN_2 peaks.

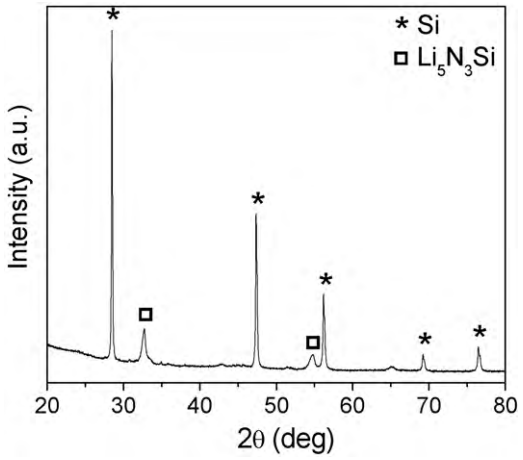

Fig. 5. X-ray diffraction data of $2LiNH_2$:Si de-hydrogenated sample.

The "*u*" value cannot be determined even if the stoichiometry of as-milled Si-sample is known because the re-hydrogenated Si-sample contains an important amount of Li_2SiN_2 and some amorphous phase (with unknown stoichiometry). If this amorphous phase has low Si content the XRD peaks are small compared to the peaks belonging to Si-rich phases. The presence of a large number of crystalline contributions makes difficult an accurate Rietveld quantitative analysis of the products of this reaction. As we will see in the following, reaction (3) accounts for doubling the plateau pressure of PCI des curve compared to that of the R-sample (reaction (1)). As a consequence, Si addition destabilizes the $LiNH_2$ + LiH system.

An attempt to obtain directly Li_2SiN_2 by ball milling and dehydrogenation of the mixture $2LiNH_2$ + Si has been performed. As indicated by the XRD patterns of Fig. 5, this sample contains Li_5N_3Si and an important amount of un-reacted Si. Consequently, in order to satisfy the reaction stoichiometry an amount of NH_3 must be released. This proves clearly that the presence of LiH is very important to avoid the release of NH_3 and the progressive loss of hydrogen storage capacity of the $LiNH_2$.

XPS spectra of the Si_{2p} core levels give a confirmation for the presence of the Li_2SiN_2 phase as shown in Fig. 6. The patterns of both re-hydrogenated (Fig. 6A) and de-hydrogenated (Fig. 6B) Si-samples show the most important peak at about 101.8 eV. This binding energy is very close to one obtained for Si_3N_4, of about 101.9 eV [14]. The peak is more intense for the de-hydrogenated sample compared to the re-hydrogenated one, in good agreement with the XRD data. A small Si bulk contribution can also be detected for both spectra. The XPS spectrum of the Si_{2p} core levels for $2LiNH_2$:Si de-hydrogenated sample (Fig. 6C) shows a broad peak and its de-convolution indicates the presence of SiO_2 and some other phases. The amount of Li_5N_3Si, as given by XRD data of $2LiNH_2$:Si de-hydrogenated sample (Fig. 5), is very small compared to the Si bulk amount. However, it is not possible to put in evidence a contribution of the Si bulk in the XPS spectrum of this sample, despite the most important contribution as shown by XRD data is pure Si. Most probable, the broad XPS peak for this sample is an overlapping of the peaks belonging to Li_5N_3Si and SiO_2 phases which are formed at the Si grains boundaries.

Thermal programmed desorption (TPD) measurements (with a ramp of 3 °C/min) under vacuum for the as-milled R-sample show an amount of almost 5 wt% H_2 released at temperatures below 300 °C. We did not exceed this temperature in order to avoid any NH_3 release. The desorption starts at about 120 °C and from 220 °C to 300 °C has a constant slope (Fig. 7A). The same type of measurement for the Si-sample (Fig. 7B) shows that desorption begins

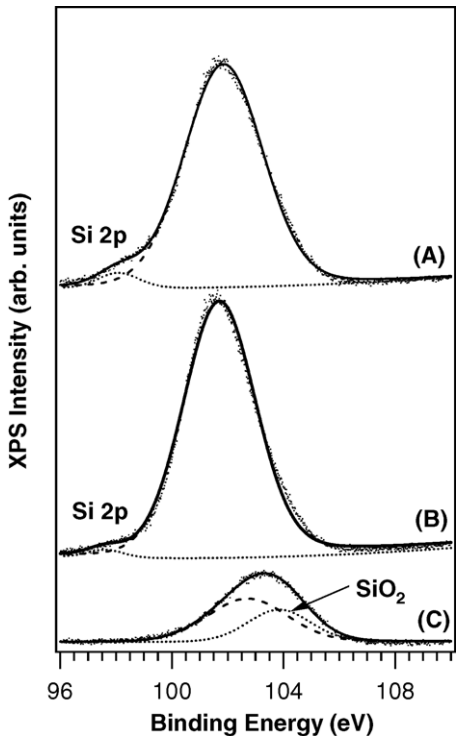

Fig. 6. XPS Si_{2p} spectra of 3LiNH:2LiH:Si (A – re-hydrogenated, B – de-hydrogenated) and $2LiNH_2$:Si de-hydrogenated (C) samples.

at about the same temperature as for of R-sample. About 2.7 wt% H_2 is released below 300 °C, but the desorption practically finishes at about 270 °C. It is evident that desorption completion for the Si-sample occurs at lower temperatures compared to the R-sample.

Fig. 8 exhibits the PCI des curves (A for R-sample, B for Si-sample) down to 0.10 bar at 265 °C. According to this plot, the maximum amount of hydrogen released by the R-sample is 2.9 wt%. The TPD curve shows an amount of 3.4 wt% H_2 desorbed below the same temperature. The reason for this discrepancy is a large plateau region (0.5 wt%) at pressures below 0.10 bar, the lowest pressure value allowed by the experimental setup for this kind of measurements (PCI des). The PCI des curve at 265 °C for the R-sample measured down to 0.10 bar has a plateau with a middle pressure of 0.60(5) bar. The Si-sample also exhibits only one plateau with a middle pressure value of 1.25(5) bar, proving a thermodynamic destabilization effect due to the Si addition, in good agreement with reaction (3). The maximum hydrogen content by weight

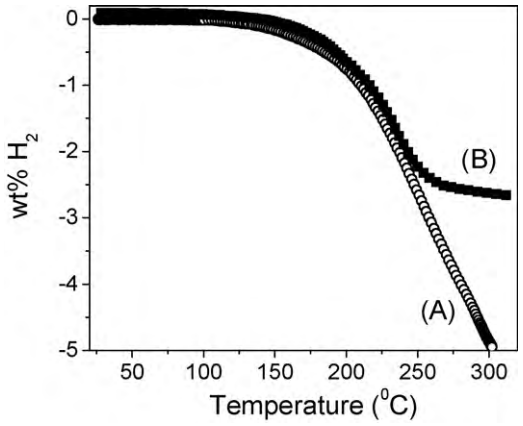

Fig. 7. Thermal programmed desorption curves of $LiNH_2$ + LiH (A) and 3LiNH:2LiH:Si (B).

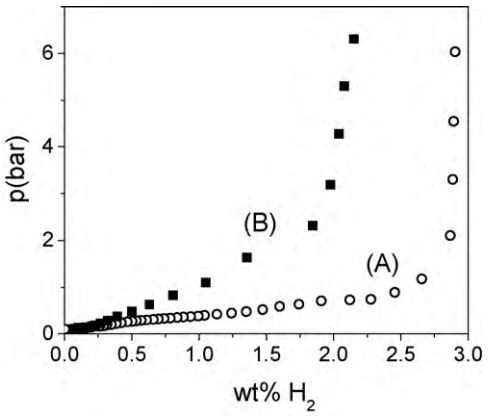

Fig. 8. Pressure–composition isotherms in desorption mode at 265 °C of $LiNH_2$ + LiH (A) and 3LiNH:2LiH:Si (B).

obtained from the PCI des curve for the Si-sample is 2.15 wt%, with 0.35 wt% lower than the 2.5 wt% released below the same temperature (265 °C) in the TPD measurement. The same reason could explain this difference, a region of the PCI curve below 0.1 atm. The $LiNH_2$:LiH system is inefficient as hydrogen storage material due to low hydrogen desorption pressure. Si addition improves to some extent this situation because 1.35 wt% H_2 is released at pressures >1 atm for the Si-sample compared to only 0.4 wt% released by the R-sample. This is only a first result proving the effectiveness of Si for the Li amide destabilization. Further extensive work is required to investigate the possible Si destabilization effect on other amides, and mixture of amides and hydrides.

4. Conclusions

$LiNH_2$:LiH and $3LiNH_2$:2LiH:Si composites were prepared by ball milling after which an increase of the lattice parameters of $LiNH_2$ was observed compared to the literature data for bulk phase, while for LiH the lattice parameter remained practically unchanged. The crystal size of the milled samples increases 2–3 times after hydrogen absorption–desorption cycles. LiH crystal size was less affected by hydrogenation. Li_2SiN_2 phase was formed for the Si-containing samples after few hydrogen absorption–desorption cycles. X-ray diffraction data proved an increase of Li_2SiN_2 and a decrease of Si amount for the de-hydrogenated Si-containing samples compared to re-hydrogenated ones. The presence of this phase was also confirmed by XPS measurements. This fact indicated a hydrogen reversible generating reaction: $(u+1)LiNH_2 + uLiH + (1/2)Si \leftrightarrow uLi_2NH + (1/2)Li_2SiN_2 + (u+1)H_2$, result also supported by PCI measurement in desorption mode. Si addition to $LiNH_2$:LiH system increased by two times the plateau pressure, resulting in a destabilization observed for the first time of $LiNH_2$:LiH system by Si addition.

Acknowledgements

Support of the Romanian Ministry of Research and Education through the project PNCDI-2 72-196/2008 "New complex hydrides for hydrogen storage in hydride tank suitable for vehicular applications"—STOHICO is strongly acknowledged.

References

[1] R. Genma, H.H. Uchida, N. Okada, Y. Nishi, J. Alloys Compd. 356–357 (2003) 358.
[2] A. Züttel, P. Wenger, S. Rentsch, P. Sudan, Ph. Mauron, Ch. Emmenegger, J. Power Sources 118 (1–2) (2003) 1.
[3] P. Chen, Z. Xiong, G. Wu, Y. Liu, J. Hu, W. Luo, Scripta Mater. 56 (10) (2007) 817.
[4] P. Chen, Z. Xiong, J. Luo, J. Lin, K. Lee Tan, Nature 420 (2002) 302.

[5] P. Chen, Z. Xiong, J. Luo, J. Lin, K.L. Tan, J. Phys. Chem. B 107 (39) (2003) 10967.
[6] Y.H. Hu, E. Ruckenstein, J. Phys. Chem. A 107 (46) (2003) 9737.
[7] J.J. Vajo, G.L. Olson, Scripta Mater. 56 (10) (2007) 829.
[8] W. Luo, J. Alloys Compd. 381 (1–2) (2004) 284.
[9] S. Barison, F. Agresti, S. Lo Russo, A. Maddalena, P. Palade, G. Principi, G. Torzo, J. Alloys Compd. 459 (2008) 343.
[10] S. Liu, L. Sun, F. Xu, Prog. Chem. 20 (2–3) (2008) 280.
[11] M.U. Niemann, S.S. Srinivasan, A. Kumar, E.K. Stefanakos, D.Y. Goswami, K. McGrath, Int. J. Hydrogen Energy 34 (19) (2009) 8086.
[12] K. Luo, Y. Liu, F. Wang, M. Gao, H. Pan, Int. J. Hydrogen Energy 34 (19) (2009) 8101.
[13] L. Lutterotti, P. Scardi, P. Maistrelli, J. Appl. Crystallogr. 25 (3) (1992) 459.
[14] L.G. Jacobsohn, R.K. Schulze, L.L. Daemen, I.V. Afanasyev-Charkin, M. Nastasi, Thin Solid Films 494 (2006) 219.